REPORT DOCUMENTATION PAGE

Form Approved
OMB No. 0704-0188

PLEASE DO NOT RETURN YOUR FORM TO THE ABOVE ADDRESS.

1. REPORT DATE *(DD-MM-YYYY)*	2. REPORT TYPE	3. DATES COVERED *(From - To)*
2007	Reprint	Aug 2006-Aug 2007

4. TITLE AND SUBTITLE

Nano-aluminum flame spread with fingering combustion instabilities

5a. CONTRACT NUMBER

W911NF-04-1-0178

5b. GRANT NUMBER

5c. PROGRAM ELEMENT NUMBER

6. AUTHOR(S)

J.Y. Malchi a,*, R.A. Yetter a, S.F. Son b, G.A. Risha a

5d. PROJECT NUMBER

5e. TASK NUMBER

5f. WORK UNIT NUMBER

7. PERFORMING ORGANIZATION NAME(S) AND ADDRESS(ES)

a The Pennsylvania State University, University Park, PA, USA
b Los Alamos National Laboratory, Los Alamos, NM, USA

8. PERFORMING ORGANIZATION REPORT NUMBER

9. SPONSORING/MONITORING AGENCY NAME(S) AND ADDRESS(ES)

U. S. Army Research Office
P.O. Box 12211
Research Triangle Park, NC 27709-2211

10. SPONSOR/MONITOR'S ACRONYM(S)

11. SPONSOR/MONITOR'S REPORT NUMBER(S)

12. DISTRIBUTION/AVAILABILITY STATEMENT

Approved for public release; federal purpose rights.

13. SUPPLEMENTARY NOTES

The views, opinions and/or findings contained in this report are those of the author(s) and should not be construed as an official

14. ABSTRACT

Three consecutive modes of flame propagation were observed over a bed of nano-aluminum burning with a counter-flowing oxidizer of 20% oxygen and 80% argon by volume, each displaying significantly different characteristics. The first mode of propagation was the focus of this study and was examined within the critical Rayleigh and Peclet number regime where three-dimensional buoyancy effects were hindered and the fingering thermal-diffusive instability occurred. Fingering flame spread was observed and characterized for various Peclet numbers, top plate heights and particle sizes to gain a better understanding of the reaction mechanism associated with the combustion of nano-particles in close contact. Results indicate that the first mode of flame propagation over a bed of nano-aluminum has spread rates an order of magnitude greater than that of cellulose fuels. However, similar trends occur when varying the Peclet number and the height of the top plate. Furthermore, faster propagation speeds occur with smaller particles because of their increased specific surface area. The widths of the fingers grow and more of the surface is burned with increasing particle size due to the longer time scale available for lateral growth.

15. SUBJECT TERMS

Flame spread; Nano-aluminum powder; Thermal-diffusive instability; Peclet number; Fingering combustion

16. SECURITY CLASSIFICATION OF:			17. LIMITATION OF ABSTRACT	18. NUMBER OF PAGES	19a. NAME OF RESPONSIBLE PERSON
a. REPORT	b. ABSTRACT	c. THIS PAGE			Richard A. Yetter
UU	UU	UU	UU	9	19b. TELEPHONE NUMBER *(Include area code)* 814-863-6375

Reset

Available online at www.sciencedirect.com
ScienceDirect
Proceedings of the Combustion Institute 31 (2007) 2617–2624
Proceedings of the Combustion Institute
www.elsevier.com/locate/proci

Nano-aluminum flame spread with fingering combustion instabilities ☆

J.Y. Malchi [a,*], R.A. Yetter [a], S.F. Son [b], G.A. Risha [a]

[a] The Pennsylvania State University, University Park, PA, USA
[b] Los Alamos National Laboratory, Los Alamos, NM, USA

Abstract

Three consecutive modes of flame propagation were observed over a bed of nano-aluminum burning with a counter-flowing oxidizer of 20% oxygen and 80% argon by volume, each displaying significantly different characteristics. The first mode of propagation was the focus of this study and was examined within the critical Rayleigh and Peclet number regime where three-dimensional buoyancy effects were hindered and the fingering thermal-diffusive instability occurred. Fingering flame spread was observed and characterized for various Peclet numbers, top plate heights and particle sizes to gain a better understanding of the reaction mechanism associated with the combustion of nano-particles in close contact. Results indicate that the first mode of flame propagation over a bed of nano-aluminum has spread rates an order of magnitude greater than that of cellulose fuels. However, similar trends occur when varying the Peclet number and the height of the top plate. Furthermore, faster propagation speeds occur with smaller particles because of their increased specific surface area. The widths of the fingers grow and more of the surface is burned with increasing particle size due to the longer time scale available for lateral growth.

Keywords: Flame spread; Nano-aluminum powder; Thermal-diffusive instability; Peclet number; Fingering combustion

1. Introduction

The high heat of reaction of aluminum formulations makes it a performance enhancer in solid rocket propellants. With nano-sized aluminum (nAl) particles, the specific surface area increases creating easier ignition and increased burn rates [1]. Nano-particles can also be mixed with metal oxide powders to create highly energetic metastable intermolecular composites (MICs) for a variety of applications. MICs can have burn rates of up to 1 km/s [2,3].

From a single particle [4–6], to an ingredient in a composite propellant [7,8], aluminum has been both modeled and studied experimentally. However, in order to gain a better understanding of its combustion properties, aluminum particles reacting in close contact is an area that needs further investigation. When a pile of nAl powder is ignited in the open atmosphere, a flame front spreads across the surface. In contrast, ignition and flame spread cannot easily be obtained with micron-sized aluminum powder. This brings up fundamental questions as to how a reaction wave spreads across nAl powder. Past flame spread studies of solid fuels have provided a controlled

☆ Supplementary data for this article can be accessed online. See Appendix A.

* Corresponding author. Fax: +1 814 865 3389.
E-mail address: jym100@psu.edu (J.Y. Malchi).

1540-7489/$ - see front matter © 2006 The Combustion Institute. Published by Elsevier Inc. All rights reserved.
doi:10.1016/j.proci.2006.08.046

manner in which to study the roles of fuel and oxidizer properties during a combustion event.

Flame spread over thermally thin and thick fuels with a counter-flowing oxidizer have been modeled [9–12] and studied experimentally [13–15]. Experiments by Fernandez-Pello *et al.* [13] show that, at low oxidizer flow velocities, the flame-spread rate over thin and thick fuels becomes practically independent of the gas velocity. It is hypothesized that at these low velocities, buoyancy-driven, three-dimensional hydrodynamics of the oxidizer start playing a role in feeding the flame.

Investigations of flame spread in microgravity with low oxidizer velocities have shown that the spread propagation velocity will continue to decrease while the continuous front begins to separate into "fingers". These fingers are a result of a thermal-diffusive instability present at these low flows [16,17]. Zik and Moses [18] were able to reproduce these instabilities in gravity by introducing a top boundary to the flow. This top plate, when brought to a critical height, or critical Rayleigh number (Ra), was able to prevent buoyancy flows and thus, create fingering instabilities in a certain Peclet number (Pe) regime. Below a critical Ra and Pe, the dimensions and spacing of the fingers could be well controlled. It was concluded that the distance between the fingers was determined by the availability of oxygen, while the width of the fingers was determined by the heat losses in the system. The propagation speed of the fingers depended on the velocity of the oxidizer and the dimensions of the fingers.

The objective for this paper is to examine the fingering flame spread of a bed of nAl powder. Utilizing nAl powder allows for investigations of other significant variables, such as particle size (d_p) and packing density (ρ_{pack}) that cannot be obtained with a single piece of solid fuel such as filter paper. Moreover, the use of fingering flame spread allows for a well-controlled experiment to give insight into the combustion of nano-aluminum particles in contact with each other.

2. Experiment

The experiment consists of a copper bottom plate, copper gas diffuser (5 in Fig. 1) and an aluminum bracket which holds the top plate. For visualization, a quartz window is used as the top plate (1 in Fig. 1). To prevent lateral flow over the bed, copper shims were placed along the sides (2 in Fig. 1). The top plate rests on the shims, thus, the height of the shims also determines the height of the top plate (h). The aluminum sits in the bed of the bottom plate (3 in Fig. 1) that has dimensions $3.81 \times 6.35 \times 0.32$ cm. Bed shims with thickness of 0.08 cm were also created to adjust the thickness of the bed (t_{bed}). The gas diffuser has oxidizer inlets on both ends and a row of twenty-four 0.08 cm diameter holes on the exit face used to distribute the flow across the width of the channel and assure uniform flow development. A nichrome wire is placed through holes at the opposite end of the bottom plate (4 in Fig. 1) and resistively heated by a DC power supply to serve as an ignition source.

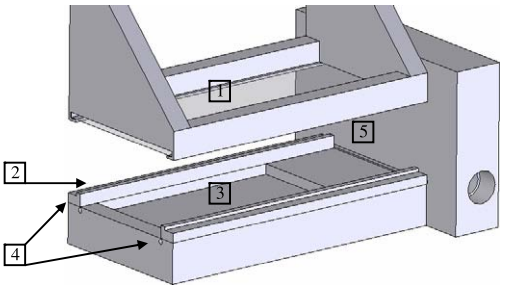

Fig. 1. Schematic of the nAl bed setup. 1. quartz top plate, 2. copper side shims, 3. bed for nAl, 4. holes for ignition wire, 5. copper gas diffuser.

To capture the experiment, a Pulnix TMC-6700-CL camera was used at 30 frames per second with a shutter time of 1/30 of a second. Each frame was scanned to find the x-location of pixels with intensities above 10% of the maximum. These values were recorded and averaged to acquire an average x-location for each frame. The average x-location and the time between each frame were used to calculate an average velocity of the front (v_f). Depending on the experimental condition, an appropriate aperture was chosen to capture enough light without saturation.

The oxidizer was a gas mixture of 20% oxygen and 80% argon by volume. To control the flow, two mass flow-controllers (Hastings HFC-202) were used (one for the oxygen and one for the argon). The oxygen fraction and flow velocity were controlled by a computer data acquisition system (Measurement Computing USB-1208FS DAQ Board and National Instruments Labview 7.1). Fluid dynamics calculations (Fluent 6.2) were performed on the extreme cases to find an adequate distance for the flow to become fully developed. The distance from the exit of the gas diffuser to the beginning of the nAl particle bed was found to be 2.5 cm to assure fully developed flow. The average oxidizer velocity (v_{ox}) was determined by the channel cross-sectional area and the oxidizer flow rate. For some experiments, the entire exhaust gas exiting from the test section was sampled and analyzed by gas chromatography (Agilent Micro GC3000) for oxygen concentration.

A pre-measured mass of nAl powder was placed in the bed and distributed uniformly. To create a smooth top surface, a glass surface was used to lightly press the powder into the bed.

Four different sized particles were used having diameters of 38 (Technology Materials Development), 50, 80, and 120 nm (latter three from Nanotechnologies, Inc.). The oxide passivation layers are 3.1, 2.1, 1.9, and 1.8 nm and the pycnometer densities are 3.2, 3.0, 3.1, and 2.9 g/cm^3, respectively. An SEM micrograph of 80 nm nAl in Fig. 2 shows the approximate spherical shape and the uniformity of the particles.

Experiments were conducted specifically to study the effects of Pe, h, and d_p on v_f, the average width of fingers (w_f), and the average distance between fingers (w_b). The Peclet number was defined as $v_{ox}h/D_{O_2}$, where D_{O_2} is the molecular diffusion coefficient of oxygen and assumed constant throughout at a value of 0.25 cm^2/s.

3. Results and discussion

We observe three modes of flame propagation (Fig. 3) that occur sequentially throughout each experiment: 1. counter-flow surface reaction wave, 2. co-flow bulk reaction wave, and 3. cellular flames randomly propagating through the material somewhat similar to what was observed by Zhang *et al.* [14] with filter paper in low Lewis number atmospheres near the extinction limit. Son *et al.* [19] observed the bottom of a pile of nAl during the first wave to confirm this was only a surface burn. This study focused on the first wave.

To demonstrate the effect of Pe and h, 38 nm particles were packed at equal ρ_{pack} of 0.22 g/cm^3 in beds with a thickness (t_{bed}) of 0.32 cm. The effect of d_p was investigated at two different Pe values and $h = 2$ mm with particle diameters of 50, 80, and 120 nm. A ρ_{pack} of 0.34 g/cm^3 was used for these experiments. Due to the inherent pouring density of the Nanotechnologies Inc. particles, a larger mass was needed to completely fill the bed. Because of a limited amount of these particles available, t_{bed} was reduced to 0.08 cm for these experiments. Experiments showed this did not affect the first wave.

Figure 4a shows a sequence of video frames ($\Delta t = 1/15$ s). The flame's trail loses luminosity a certain distance behind the front. This trail length is the order of 1 mm long. Integration of all of the frames along the whole length of the bed (Fig. 4b) shows the history of the flame spread. Along with Fig. 4b, Fig. 5 shows flame histories for a bed of 38 nm particles for $Pe = 3$, 9, and 16 at $h = 2$ and for $h = 2$, 6, and 10 mm at $Pe = 3$.

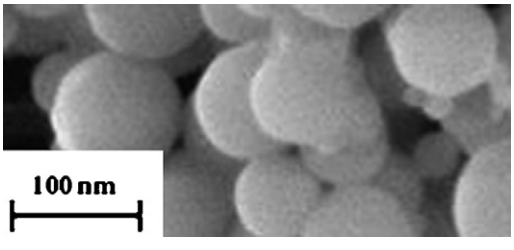

Fig. 2. SEM micrographs of 80 nm aluminum particles manufactured by Nanotechnologies, Inc.

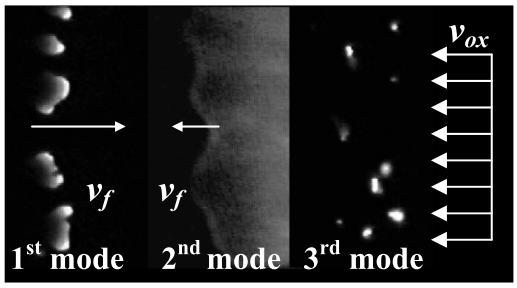

Fig. 3. Three modes of combustion for a bed of 38 nm nAl.

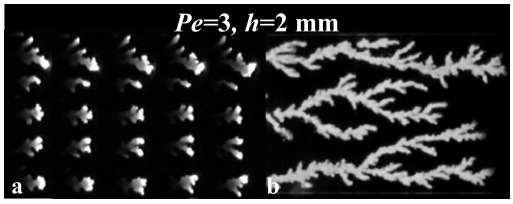

Fig. 4. (a) Sequence of frames each 1/15 s apart (b) all frames integrated through the run to show the history of the flame spread for a 38 nm nAl bed.

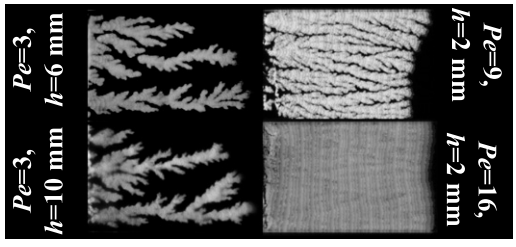

Fig. 5. Integrated flame histories of beds of 38 nm nAl. Refer to Fig. 4b for a Peclet number (Pe) of 3 and top plate height (h) of 2 mm case.

3.1. Conservation of mass

Analysis of the exhaust gases by gas chromatography at the exit during the first wave showed an oxygen concentration of 0.8%, a 96% decrease from the original amount. It is reasonable to assume in the analysis that all of the oxygen is consumed by the front and a global mass conservation can be written as

$$\Gamma_{Al} = \mu_{stoic}\Gamma_{O_2}, \quad (1)$$

where Γ_{Al} is the mass consumption rate of aluminum per unit area, Γ_{O_2} is the mass consumption rate of oxygen per unit area and μ_{stoic} is the stoichiometric coefficient.

When varying the height of the top plate, *Pe* is kept constant. Therefore, the mass flow rate per unit area of oxidizer ($\dot{m}''_{ox}$) and, thus, Γ_{O_2} are constant. Since Γ_{O_2} is constant, Γ_{Al} must be equal for each case according to Eq. (1).

For the $Pe = 3$, $h = 6$ mm and $Pe = 3$, $h = 10$ mm cases the first 40% of the burn is neglected. Notice from Fig. 5 that this area contains noticeably more burned surface area than the latter 60%. At these Peclet numbers, the v_{ox} is relatively slow. The slow velocity could possibly allow a small amount of air to diffuse through the open end at the exit of the apparatus. An order of magnitude analysis shows that this could only have a small effect, but preliminary experiments with no oxidizer flow also show this phenomenon. Moreover, since the oxygen is being consumed, the gas pressure will decrease after the front creating a pressure gradient that could induce flow in from the ambient at a higher rate than estimated by diffusion. These observations could also be an initial transient for the instability that is exaggerated by the high top plate heights and low advective flows.

The Γ_{Al} is calculated using

$$\Gamma_{Al} = f_b \rho_{Al_{bed}} v_f \delta_b, \quad (2)$$

where $\rho_{Al_{bed}}$ is the packing density of just the aluminum in the bed (ρ_{pack} without oxide layer), f_b is the fraction of surface area burned, and δ_b is the non-dimensional depth of burned aluminum scaled by a particle diameter ($\delta_b = d_p/d_{ref}$ where d_{ref} is a reference depth of 50 nm, a typical nAl particle size). A non-dimensional depth is used because the depth of the burn is not known for this experiment. It is assumed, however, that the particles lined up directly on top of each other and the depth of the burn scaled with the diameter of the particle. The Γ_{Al} was found to be 0.42, 0.43, and 0.49 g/cm^2-s for h of 2, 6, and 10 mm, respectively. The Γ_{Al} for $h = 10$ is slightly higher due to the slowest oxidizer velocity further exaggerating the initial transient discussed above.

When varying *Pe*, h is kept constant. As *Pe* increases, Γ_{Al} should increase accordingly. Equation (1) can be simplified to $f_b v_f = Z v_{ox}$, where Z is a constant equal to $\mu_{stoic}\rho_{O_2}\Delta_{ox}/\rho_{Al_{bed}}\delta_b$, Δ_{ox} is the non-dimensional height of the oxidizer flow channel ($\Delta_{ox} = h/h_{ref}$ where h_{ref} is a reference height of 2 mm, the lowest h used in the experiment), and ρ_{O_2} is the density of oxygen. Therefore, v_f multiplied by f_b should vary linearly with the velocity of the oxidizer as shown in Fig. 6.

The values of $\rho_{Al_{bed}}$ are found to be 0.29, 0.26, and 0.24 g/cm^3 for d_p of 50, 80, and 120 nm, respectively. The Γ_{Al} can be found for each case at the same *Pe* and compared using Eq. 2. For $Pe = 3$, $\Gamma_{Al} = 0.06$, 0.07, and 0.06 g/cm^2-s for $d_p = 50$, 80, and 120 nm, respectively. For $Pe = 5$, $\Gamma_{Al} = 0.16$, 0.11, and 0.13 g/cm^2-s for $d_p = 50$, 80, and 120 nm, respectively.

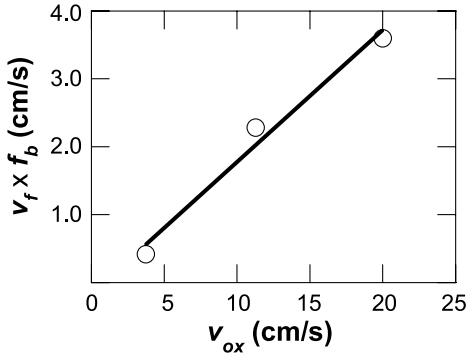

Fig. 6. Relation between the flame propagation velocity (v_f) and the oxidizer velocity (v_{ox}) for varying the Peclet number (*Pe*).

3.2. Effect of top plate height

Figure 7 shows the trends for w_f, w_b, and f_b at a constant value of $Pe = 3$ with a varying h value. Since the *Pe*, and thus, the mass flow rate per unit area of oxygen ($\dot{m}''_{O_2}$) are constant, the f_b remains nearly constant as well. There is a significant increase in w_f with an increase in h, while w_b remains nearly constant. From the conservation of mass analysis above, v_f must stay constant as is shown in Fig. 8. Overall, when h increases, v_{ox} must decrease to keep *Pe* constant. With a slower v_{ox} and a higher h the flame front losses some ability to conduct heat out through the top plate due to a decreasing convective flow and an increase in the length scale for conduction. This loss of ability for the front to conduct heat out through the top results in an increase in w_f. To compensate for the

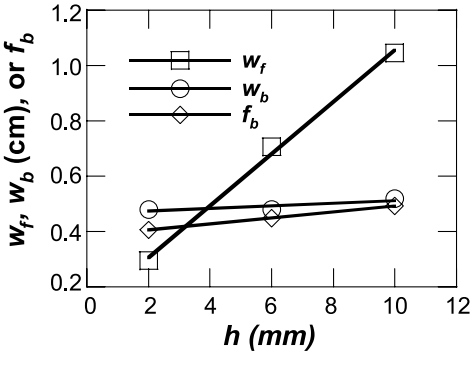

Fig. 7. Trends for the width of the fingers (w_f), width between the fingers (w_b), and the fraction burned (f_b) at Peclet number (*Pe*) of 3 for 38 nm nAl bed.

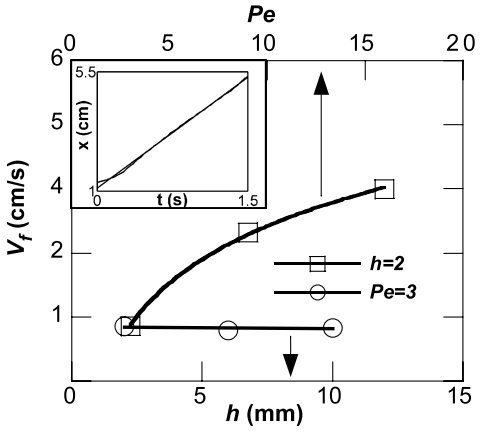

Fig. 8. Trend for flame propagation velocity (v_f) with varying top plate height (h) or Peclet number (Pe) for 38 nm nAl bed; insert shows the steady nature of the front.

increase in w_f, fewer fingers are present with practically constant values of w_b, f_b, and v_f. The average flame front velocity is constant throughout the run as shown in the insert in Fig. 8. Each finger will remain at a velocity nearly equal to the overall average v_f if it is undisturbed. However, if a finger propagates in front of another it will "screen" the finger from the oxygen and extinguish it.

3.3. Effect of Peclet number

Figure 9 shows that f_b increases as Pe increases, which results from the increase in $\dot{m}''_{O_2}$ of the oxidizer stream. For the $Pe = 3$ and $Pe = 9$ cases, w_f was found nearly constant increasing only slightly from 3 and 5 mm, respectively. The work of Zik *et al.* [18] showed this trend as well with filter paper for a constant h. Since these conditions have nearly constant values of w_f, w_b must decrease when f_b increases as is shown in Fig. 9. At $Pe = 16$, a nearly flat front is observed forcing

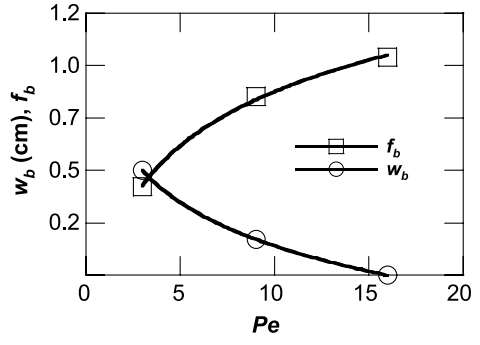

Fig. 9. Trends for the fraction burned (f_b) and the width between the fingers (w_b) at a top plate height (h) of 2 mm for 38 nm nAl bed.

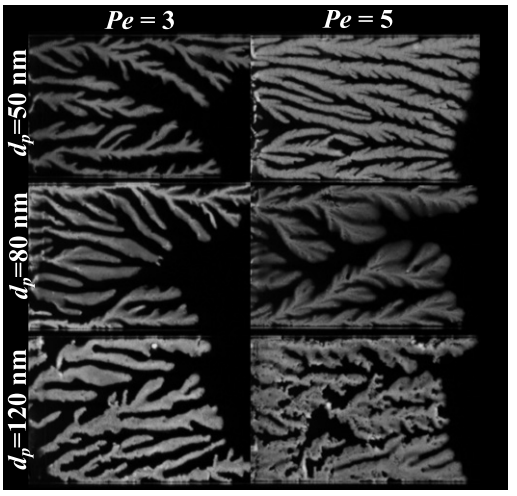

Fig. 10. Integrated flame spread histories for different particle diameters (d_p) at Peclet numbers (Pe) of 3 and 5 and a top plate height (h) of 2 mm.

w_f to be the width of the bed, w_b to be zero, and the total surface area to be consumed. For this condition, the critical Pe, which is a threshold value where the fingering instability ceases to occur, has been exceeded. Figure 8 shows that v_f increases significantly with increasing Pe. This increase is directly related to the conservation of mass analysis for increasing Pe.

3.4. Effect of particle size

Figure 10 shows integrated histories of the flame spread for 50, 80, and 120 nm at $Pe = 3$ and $Pe = 5$. Since smaller aluminum has a higher specific surface area, the burn time for particles will decrease with decreasing diameter, which should lead to faster front velocities for beds of

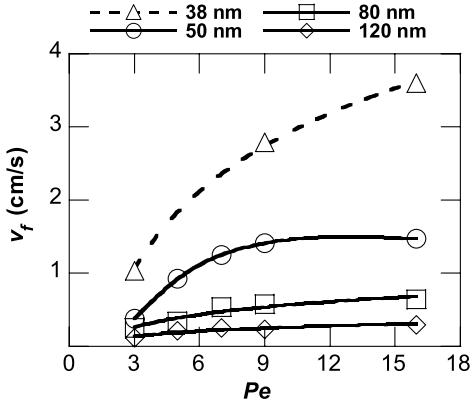

Fig. 11. Trend for flame propagation velocity (v_f) with varying Peclet number (Pe) for different particle diameters (d_p) at a top plate height (h) of 2 mm.

smaller particles. These velocities are shown in Fig.11. The data from the 38 nm cases further demonstrate this trend even though these particles have a larger oxide passivation layer, lower ρ_{pack}, and a larger t_{bed}.

Changing the particle size will also have an effect on w_f and f_b. Since a bed of smaller particles will propagate faster due to the higher specific surface area, the f_b must decrease according to Eq. (2). This trend is shown in Fig. 12. For the larger particles, the slower front velocities allow more time for the lateral diffusion of the flame causing wider fingers. Furthermore, because there are fewer particles per bed for the same ρ_{pack}, larger particle sizes will have less contact resistance. This will lead to a higher thermal conductivity, which could aid in the widening of the fingers.

3.5. Other observations and future work

Notice in Fig. 11, v_f becomes independent of Pe (or v_{ox}) at $Pe > 9$ for the slower burning particles. At these higher values of Pe the whole surface of the nAl bed is burned ($f_b \rightarrow 1$, and $w_b \rightarrow 0$). Thus, the mass of oxygen available begins to exceed the stoichiometric value and not all of it is consumed by the front. Therefore, the front is "saturated" and has reached a maximum v_f. This independence of oxidizer velocity indicates that the nAl bed is thermally thin according to deRis' [9] model of opposed flow flame spread. However, v_f is also independent of t_{bed}, as described above, indicating that the bed is thermally thick [9]. The explanation for this contradiction is that the whole bed is not participating in the first wave. It can be considered a thermally thin flame spread resting on top of a non-participating bed of fuel.

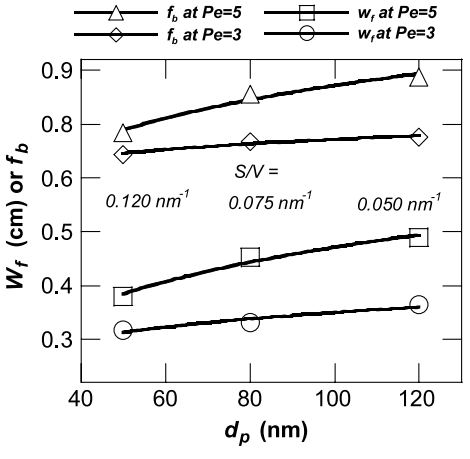

Fig. 12. Trends for the width of the fingers (w_f) and fraction burned (f_b) with varying particle diameters (d_p) or surface to volume ratios (S/V) at two different Peclet numbers for a top plate height (h) of 2 mm.

The integrated histories of each particle size displayed distinct fingering patterns at certain Peclet numbers. Figure 10 shows the experiments with $Pe = 3$ having similar structures. However, with $Pe = 5$, the fingers look significantly different depending on d_p. The 80 nm particle bed has fingers that have a feathery look, for example. The branches are wider than the 50 nm particle bed and the edges have a much smoother intensity gradient. The 120 nm particle bed has fingers that are not well defined and the edges are extremely jagged.

During some runs, the front seems to jump forward as shown in Fig. 13. This could be an example of an agglomeration of particles exploding and propelling the hot products forward. Particle explosion was observed by Yetter *et al.* [4] for single particles. More frequent explosions of this magnitude were noticed with smaller particles at higher propagation velocities, although this mode of propagation is the exception.

An experiment was performed with no top plate and slow v_{ox}. With no top plate, three-dimensional buoyancy effects are not suppressed and the existence of fingers would not be anticipated based on previous experiments with filter paper combustion. However, fingers are present even without a top plate, which could be due to a faster v_f for nAl than for filter paper allowing less time for buoyancy flow to develop. There was, however, more surface area burned, more fingers and a faster v_f than with the top plate indicating that the restricted buoyant flow from the top plate does play a significant role in the fingering behavior. The induced buoyant flow causes v_f and the finger dimensions to be similar to a run with $Pe = 9$.

After the first and second waves, no white alumina powder was observed, which is what would be expected if stoichiometric Al_2O_3 is formed. Only after the third mode were trails of white noticed. It is hypothesized that the first wave only thickens the already present Al_2O_3 layer a small amount (possibly changing its polymorph structure) to remain optically thin and, therefore, the particles do not appear white in color, but are slightly discolored from the unburned bed. The second wave could leave the particles optically thin as well, or since it is diffusion limited, there could be non-stoichiometric products formed.

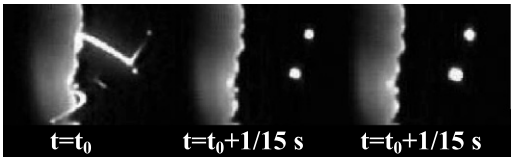

Fig. 13. Example of particle(s) explosion in 80 nm nAl bed.

4. Conclusions

Flame spread was examined over a bed of nAl particles with 20% O_2 and 80% Ar, by volume, as the oxidizer. Similar to the experiment of Zik *et al.* [18], a top plate was used to inhibit three-dimensional buoyancy effects and create a fingering instability that was only observed in flame spread experiments in microgravity. This gave insight into the nature of nano-aluminum particles burning in close contact with each other.

Specifically, we found:

1. Three flame propagation modes are observed over a bed of nAl with an opposed oxidizer flow, including a discrete cellular flame mode.
2. The first mode of flame propagation across a bed of nano-aluminum particles was investigated in this study and has similar characteristics to a continuous solid fuel, although the spread rate is much more rapid.
3. For an increasing Peclet number, the width between the fingers decreases, the percent burned of surface area increases, and the propagation velocity increases.
4. For an increasing top plate height, the width between the fingers remains constant, the width of the fingers increases, and the propagation velocity remains constant.
5. Increasing particle size decreases the propagation velocity and widens the fingers. The decreased propagation velocity is due to the lower specific surface area of the particles. Because of this decreased propagation velocity, the fingers have more time to diffuse laterally creating wider fingers. Furthermore, the higher thermal conductivity of larger particle beds likely aids in the lateral diffusion of the flame.
6. The flame history, particularly at higher Peclet numbers, showed distinct finger shapes depending on the size of the particle.
7. Particles, or perhaps groups of particles, were observed to explode causing the front to jump ahead in certain areas.
8. Removing the top plate did not eliminate the fingering in contrast to filter paper flame spread. The flame spread rate and finger dimensions were similar to that of a run at a Peclet number of 9.

Acknowledgments

This work was sponsored by the US Army Research Office under the Multi-University Research Initiative under Contract No. W911NF-04-1-0178. The support and encouragement provided by Dr. David Mann and Dr. Kevin L. McNesby are gratefully acknowledged. S.F.S. is supported by Los Alamos National Laboratory (LANL), which is operated by the University of California for the US Department of Energy under the contract *W-7405-ENG-36*. The authors thank personnel at LANL, specifically Mr. Ed Roemer for the SEM micrographs of the particles and Mr. Eric Sanders for supplying the 38 nm aluminum particles.

Appendix A. Supplementary data

Supplementary data associated with this article can be found in the online version at doi:10.1016/j.proci.2006.08.046.

References

[1] K.K. Kuo, G.A. Risha, B.J. Evans, E. Boyer, *Mat. Res. Soc. Symp. Proc.* 800 (2004) 3–14.
[2] B.S. Bockmon, M.L. Pantoya, S.F. Son, B.W. Asay, J.T. Mang, *Journal of App. Phys.* 98 (6) (2005) 64903–64910.
[3] B.W. Asay, S.F. Son, J.R. Busse, D.M. Oschwald, *Prop. Expl. Pyrotech.* 29 (4) (2004) 216–219.
[4] R.A. Yetter, P. Bucher, F.L. Dryer, *Proc. Combust. Inst.* 26 (1996) 1899–1908.
[5] M.A. Trunov, M. Schoenitz, E.L. Dreizin, in: 2005 Joint Meeting of the U.S. Sections of the Combust. Inst.
[6] K. Park, A. Rai, D. Mukherjee, M.R. Zachariah, *J. Phys. Chem. B* 109 (2005) 7290–7299.
[7] G.V. Ivanov, F. Tepper, in: K.K. Kuo (Ed.), *Challenes in Propellants and Combustion 100 Years after Nobel*, Begell House, 1997, pp. 636–645.
[8] M.M. Mench, C.L. Yeh, K.K. Kuo, in: Proc. Of the 29th Annual Conf. ICT (1998) 30–15.
[9] J.N. deRis, *Proc. Combust. Inst.* 12 (1969) 241–252.
[10] P.H. Thomas, *Combust. Sci. Tech.* 28 (1982) 173–184.
[11] S. Wichman, F.A. Williams, *Combust. Sci. Tech.* 33 (1983) 207–214.
[12] M.A. Delichatsios, *Proc. Combus. Inst.* 26 (1996) 1495–1503.
[13] A.C. Fernandez-Pello, S.R. Ray, I. Glassman, *Proc. Combust. Inst.* 18 (1981) 579–587.
[14] Y. Zhang, P.D. Ronney, E.V. Roegner, J.B. Greenberg, *Combust. Flame* 90 (1992) 71–83.
[15] I.S. Wichman, *Prog. Energy Combust. Sci.* 18 (1992) 553–593.
[16] L.M. Oravecz, I.S. Wichman, S.L. Olson, *Proc. ASME Heat Trans. Div.* 4 (1999) 183–187.
[17] S.L. Olson, U. Hegde, S. Bhattacharjee, J.L. Deering, L. Tang, R.A. Altenkirch, *Comb. Sci. Tech.* 176 (2004) 557–584.
[18] O. Zik, E. Moses, *Phys. Rev. E* 60 (1) (1999) 519–531.
[19] S.F. Son, R.C. Dye, J.R. Busse, M.M. Sandstrom, M.T. Janicke, in: JANNAF Combustion Subcommittee Meeting, Colorado Springs, December, 2003.

Comment

Andrew Sullivan, Australian National University, Australia. Did you try initial flame spread in the same direction as oxidizer (forward flow) and would you expect to see different behavior regarding fingering?

Note: fingering resembles dendritic behavior of some cellular automata of diffusion limited aggregation modeling.

Reply. I did not try concurrent flame spread, however, Olson et al. [1] performed this in a similar experiment with paper and found that the fingers moved back and forth laterally, had a less distinct shape, burned more of the fuel surface, and had a lower steady state velocity. I would expect this to be similar with nano-aluminum because it is attributed solely to hydrodynamic effects which are similar for the two systems.

Thank you for the comment on similarity to cellular automata of diffusion limited aggregation modeling. In [2], they relate this phenomenon to electrochemical deposition, another form of diffusion limited growth of fingers.

References

[1] S.L. Olson, F.J. Miller, I.S. Wichman, *Comb. Theory and Mod.* 10 (2) (2006) 323–347.
[2] O. Zik, E. Moses, *Phys. Rev. E* 60 (1) (1999) 519–531.